Journal of Catalysis 276 (2010) 141–151

Contents lists available at ScienceDirect

Journal of Catalysis

journal homepage: www.elsevier.com/locate/jcat

Transient mechanistic study of the gas-phase HCl oxidation to Cl_2 on bulk and supported RuO_2 catalysts

Miguel A.G. Hevia [b], Amol P. Amrute [a], Timm Schmidt [c], Javier Pérez-Ramírez [a,*]

[a] Institute for Chemical and Bioengineering, Department of Chemistry and Applied Biosciences, ETH Zurich, HCI E 125, Wolfgang-Pauli-Strasse 10, CH-8093 Zurich, Switzerland
[b] Institute of Chemical Research of Catalonia (ICIQ), Avinguda dels Països Catalans 16, 43007 Tarragona, Spain
[c] Bayer MaterialScience AG, PUR-PTI-PRI, New Processes Isocyanates, Chempark B598, D-41538 Dormagen, Germany

ARTICLE INFO

Article history:
Received 12 May 2010
Revised 3 August 2010
Accepted 8 September 2010
Available online 8 October 2010

Keywords:
Deacon process
HCl oxidation
Chlorine
RuO_2
TiO_2
Rutile
Chlorination
Oxychloride
Mechanism
TAP reactor

ABSTRACT

The oxidation of HCl to Cl_2 (Deacon process) was studied over RuO_2-based catalysts in bulk and supported forms. RuO_2 (7 wt.%) was incorporated onto different TiO_2 carriers (rutile, anatase, and P25) by deposition–precipitation of $Ru(OH)_2$ followed by calcination. RuO_2/TiO_2-rutile exhibits the highest activity at ambient pressure in a continuous flow fixed-bed reactor. Insights into the mechanism of this experimentally demanding reaction on RuO_2 and the influence of the TiO_2-rutile carrier were gained by studies in the Temporal Analysis of Products (TAP) reactor at 623 K. HCl multipulsing in the absence of O_2 leads to chlorination of the catalysts with no detectable gas-phase Cl_2 production. The chlorine uptake of RuO_2 amounts to 0.16 mmol Cl g_{cat}^{-1}, which enables to estimate that *ca.* 75% of the total surface Ru atoms (coordinatively unsaturated and bridge sites) are chlorinated, forming a $RuO_{2-x}Cl_x$ oxychloride. RuO_2 is also chlorinated by Cl_2, but to a lesser extent compared to HCl. The chlorine uptake of fresh RuO_2/TiO_2-rutile per gram of sample was four times higher than that of fresh RuO_2, namely due to chlorination of the high surface area carrier. Upon equilibration at ambient pressure under Deacon conditions, the TAP-derived chlorine uptake in the supported catalyst experienced a 6-fold decrease with respect to the fresh sample due to permanent chlorination. Pulsing of a mixture of O_2 and HCl over the catalysts revealed that both gas-phase Cl_2 evolution and H_2O desorption are impeded processes. Pump–probe experiments of O_2 and HCl evidenced the tight dependence of the net Cl_2 production on both the oxygen and chlorine coverage. In addition, a limited contribution of lattice surface species could be detected by the production of small amounts of Cl_2 at very low coverages. The equilibration procedure (ambient or TAP conditions) influences the reaction mechanism and the net Cl_2 production, giving account of the reaction complexity due to the highly dynamic state of the catalyst surface. The Deacon process on $RuO_{2-x}Cl_x$-based catalysts can be mostly described by a Langmuir–Hinshelwood scheme with a minor 2D Mars–van Krevelen contribution.

1. Introduction

Chlorine is used extensively in organic and inorganic chemistry as an oxidizing agent and in substitution reactions, leading to a wide range of industrial and consumer products. More than 95% of the annual chlorine production worldwide (~50 Mton) is achieved by electrolysis in mercury, diaphragm, and membrane cells (chlor-alkali process). Upon use, 50% of the Cl_2 ends up as HCl or chloride salts [1]. HCl is environmentally undesirable and has a limited market. Consequently, there has been a growing interest in finding efficient methods for converting the HCl by-product in waste streams back into Cl_2. An attractive route for chlorine recycling is the gas-phase catalytic oxidation of hydrogen chloride with air or oxygen. This process was industrialized by Henry Deacon more than 140 years ago in the presence of a copper chloride catalyst [2,3].

Contemporary industrial processes for Cl_2 production *via* HCl oxidation in fluidized-bed reactors, such as the Shell's Shell-Chlor ($CuCl_2$–KCl/SiO_2 catalyst) [4,5] and the Mitsui's MT-Chlor (Cr_2O_3/SiO_2 catalyst) [6–8], were abandoned due to limited HCl conversion, rapid loss of activity due to volatilization of the active phase above 700 K, and corrosion issues due to the presence of unreacted HCl and product H_2O. A decade ago, Sumitomo Chemicals patented a process for HCl oxidation to Cl_2 in a multi-tubular fixed-bed reactor using supported RuO_2 catalysts [9]. The Sumitomo's process enables chlorine recycling from HCl at a relatively low temperature (preferably 473–653 K) with high conversion yields up to 90% and low energy cost in comparison with electrolysis [10]. A single reactor unit can produce 400 kton Cl_2 annually [11].

Although several carriers were considered suitable to deposit the active RuO_2 phase (TiO_2, ZrO_2, Al_2O_3, SiO_2, and the corresponding

* Corresponding author. Fax: +41 44 633 1405.
E-mail address: jpr@chem.ethz.ch (J. Pérez-Ramírez).

0021-9517/$ - see front matter © 2010 Elsevier Inc. All rights reserved.
doi:10.1016/j.jcat.2010.09.009

mixed oxides) [9], later publications in the patent [10] and in the open [11,12] literature specified that the use of TiO_2-rutile is optimal. Due to lattice matching of both active phase and support (rutile structure), RuO_2 experiences epitaxial growth as a film on top of TiO_2-rutile, giving rise to remarkable activity and stability in the Deacon process [11,12]. Besides, RuO_2/TiO_2-rutile has a high thermal conductivity, which reduces the formation of hot spots within the catalyst bed and makes it suitable for fixed-bed reactor technology.

Recent studies using surface science techniques and Density Functional Theory simulations [13–16] have given account on the mechanism of HCl oxidation over the RuO_2(1 1 0) model surface. This is the most stable facet of ruthenium dioxide and has been widely employed in oxidation studies of other substrates such as CO [17] and NH_3 [18]. Over et al. [14,15] concluded that the oxidation of HCl with atomic O producing Cl_2 and H_2O proceeds on the chlorine-stabilized RuO_2(1 1 0) surface *via* a one-dimensional Langmuir–Hinshelwood mechanism along rows of under-coordinated ruthenium sites (Ru_{cus}). The robustness of Sumitomo's catalyst was linked to the formation of a stable oxychloride, $RuO_{2-x}Cl_x$(1 1 0), resulting from the replacement of surface bridge O atoms by Cl atoms. The recombination of two adjacent surface chlorine atoms in cus positions to gas-phase Cl_2 was denoted as the rate-determining step. DFT calculations [13,14] concluded that chlorine recombination is the most energy-demanding step of the reaction on RuO_2(1 1 0). Alternatively, a recent DFT study by Studt et al. [16] concluded that the dissociative chemisorption of oxygen can be used as a single descriptor to identify active catalysts for the Deacon process, and RuO_2 is close to the top of the derived volcano curve.

Further mechanistic understanding of the Deacon process requires studies with practical catalysts, that is, using specimens of polycrystalline nature and also addressing the role of the carrier. However, suitable techniques are required to investigate this experimentally demanding reaction. In this study, several RuO_2/TiO_2 catalysts were evaluated in a fixed-bed reactor under relevant Deacon conditions (ambient pressure and high HCl concentration). The rutile polymorph was the most efficient carrier. Mechanistic studies of HCl oxidation over RuO_2, TiO_2-rutile, and RuO_2/TiO_2-rutile (in fresh and equilibrated forms) were carried out in the Temporal Analysis of Products (TAP) reactor [19–22]. This transient and time-resolved method is a powerful tool to study Deacon chemistry, enabling: (i) to quantify the chlorination of the samples by HCl or Cl_2, (ii) to assess the interaction of reactant and product molecules with the catalysts and the support, (iii) to monitor product formation (Cl_2 and H_2O), and (iv) to analyze the influence of both the oxygen and chlorine coverage on the Cl_2 production. The conclusions of this study can be conciliated with previous surface science and DFT studies and led to an improved understanding of this complex reaction over practical catalysts.

2. Experimental

2.1. Catalyst preparation and characterization

The starting compounds were $RuCl_3{\cdot}3H_2O$ (Aldrich, 99.98%), RuO_2 (Aldrich, 99.9%), TiO_2-rutile (nanopowder, Aldrich, 99.5%), TiO_2-anatase (nanopowder, Aldrich, 99.7%), and TiO_2-P25 (Aeroxide®, Evonik-Degussa). Henceforth, the notation of the pure TiO_2 polymorphs contains the letter R and A for rutile and anatase, respectively. Prior to use, the as-received oxide powders were calcined in static air at 773 K (10 K min^{-1}) for 5 h. Supported RuO_2 catalysts with a nominal ruthenium content of 7 wt.% were prepared by deposition–precipitation of $Ru(OH)_2$. The support (5 g) was dispersed in distilled water (250 cm^3) under continuous stirring. Then, an appropriate amount of $RuCl_3{\cdot}3H_2O$ dissolved in 50 cm^3 of distilled water was added to the previous slurry. Precipitation of $Ru(OH)_2$ was attained by adding drop-wise an aqueous NaOH solution (10 wt.%) to the slurry until pH 12. The suspension was kept at room temperature for 1 h and then heated to 338 K for 1 h under stirring. The suspension was cooled down, filtered, washed with distilled water until pH neutral, dried at 393 K, and calcined in static air at 773 K (10 K min^{-1}) for 5 h.

The ruthenium content in the supported catalysts was determined by Inductively Coupled Plasma–Optical Emission Spectroscopy (ICP–OES) (Perkin Elmer Optima 3200RL). Powder X-ray diffraction (XRD) was measured in a Siemens D5000 diffractometer with Bragg–Brentano geometry and Ni-filtered Cu Kα radiation (λ = 0.1541 nm). Data were recorded in the range 10–70° 2θ with an angular step size of 0.05° and a counting time of 8 s per step. Transmission electron microscopy (TEM) was carried out in a JEOL JEM 1011 microscope operated at 100 kV. Nitrogen isotherms at 77 K were recorded in a Quantachrome Autosorb-1MP gas adsorption analyzer. Prior to the measurement, the samples were degassed in vacuum at 573 K for 10 h. Temperature-programmed reduction with hydrogen (H_2-TPR) was measured in a Thermo TPDRO 1100 unit equipped with a thermal conductivity detector. The sample was loaded in the quartz micro-reactor (11 mm i.d), pretreated in He (20 cm^3 STP min^{-1}) at 393 K for 1 h, and cooled to 323 K in He. The analysis was carried out in a mixture of 5 vol.% H_2 in N_2 (20 cm^3 STP min^{-1}), ramping the temperature from 323 to 1173 K at 10 K min^{-1}.

2.2. Catalytic tests

The catalytic oxidation of HCl with O_2 was studied at ambient pressure in a quartz fixed-bed reactor (8 mm i.d.) using a sample amount of 0.5 g (particle size 200–300 μm) and a total flow of 166 cm^3 STP min^{-1}. The bed height was ~10 mm. The general flow-sheet and details of the set-up are shown in Fig. 1. The individual gases were introduced to the reactor by means of digital mass-flow controllers. The material of all the lines in the set-up was Teflon® in order to prevent corrosion problems, particularly downstream of the reactor. During the tests, the catalyst bed temperature was continuously recorded with a Fluke Digital Multimeter (model 187) equipped with a K-type thermocouple. The feed mixture contained 20 vol.% HCl and 40 vol.% O_2, balanced in N_2 (referred to as 'Deacon mixture'). Hydrogen chloride (Praxair, purity 3.0 and water content <50 ppm), oxygen (Air Products, purity 5.2), and nitrogen (Air Products, purity 5.2) were used without further purification. Two protocols were applied for catalytic evaluation. Temperature-programmed reaction was carried out by ramping the furnace temperature in the Deacon mixture from 333 to 723 K at 10 K min^{-1}. The steady-state activity of selected supported catalysts was studied by isothermal tests at 573 K for 18 h. The sample was heated in N_2 to the reaction temperature followed by introduction of the Deacon mixture. The resulting sample is hereafter referred to as chlorinated or equilibrated (e) catalyst.

On-line chlorine analysis was carried out using a miniature fiber optic spectrometer (Ocean Optics, USB2000-UV–VIS). Spectra were collected in the wavelength range of 200–600 nm every 10 s using a DT-MINI-2-GS Deuterium Tungsten Halogen Light Source and a high-sensitivity Sony ILX511 2048-element linear silicon CCD-array detector upgraded for working in the UV spectral region. The product gas passed through a Z-flow cell adopted as a flow injection analysis (FIA) type assembly having a 10-mm optical path length (FIAlab instruments). The carrier gas (N_2) provided a reference spectrum in optical absorbance processing. Water produced in the reaction was condensed using a reflux unit prior to the detection cell. Cl_2 quantification in isothermal tests was carried out by titration. The chlorine concentration at the reactor outlet

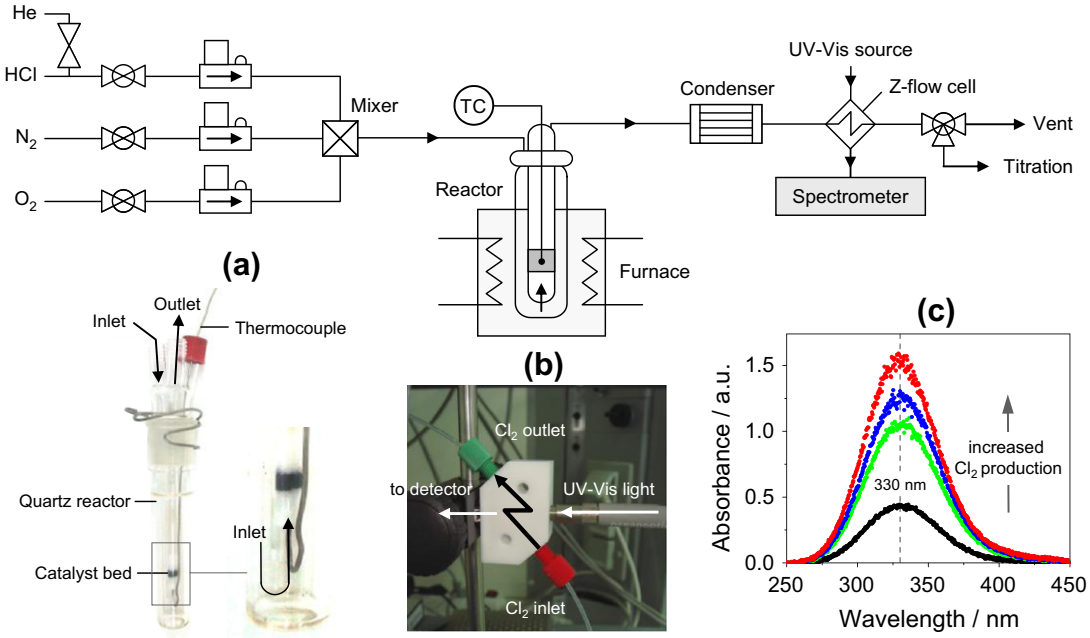

Fig. 1. Scheme of the set-up for catalytic tests: (a) fixed-bed reactor, (b) Z-flow cell, and (c) UV/Vis spectra collected at increasing chlorine production. The band centered at 330 nm is due to Cl_2.

was determined after passing through two serial impingers for 10 min, each of which equipped with a porous frit immersed into an aqueous solution of potassium iodide (2 wt.%). The thus obtained iodine was titrated with sodium thiosulfate (0.01 M). The catalytic activity was expressed by the space time yield (STY), defined as gram of Cl_2 produced per gram of catalyst and per hour.

2.3. Temporal Analysis of Products

Transient mechanistic studies were carried out in the TAP-2 reactor [19–22] over fresh RuO_2, TiO_2-R, and RuO_2/TiO_2-R, and equilibrated RuO_2/TiO_2-R-e derived from the 18-h isothermal test in the Deacon mixture (Section 2.2). The sample (10 mg, particle size 200–300 μm) was packed in the isothermal zone of the quartz micro-reactor (4.6 mm i.d.) between two layers of quartz particles of the same sieve fraction. The thickness of the catalyst zone (0.9–1.2 mm) was very small compared to the overall length of the bed (71 mm). In this configuration, referred to as thin-zone reactor, concentration gradients across the catalyst bed can be neglected [23]. The samples were pretreated in 20 cm^3 STP min^{-1} of O_2 (RuO_2, TiO_2-R, and RuO_2/TiO_2-R) or He (RuO_2/TiO_2-R-e) at 623 K and ambient pressure for 1 h. The samples were evacuated to 10^{-5} Pa, and the following pulse experiments were carried out at 623 K using a pulse size of *ca.* 10^{16} molecules:

(a) Pulses of O_2:Ar, HCl:Kr, and Cl_2:Kr (molar ratio = 2:1).
(b) Multipulses of HCl:Kr = 8:1 or Cl_2:Kr = 8:1. These experiments enable to quantify the chlorine uptake by the catalysts. Saturation was reached when the ratio between the areas of HCl or Cl_2 and Kr at the reactor outlet by MS analysis was constant.
(c) Pulses of HCl:O_2:Kr = 2:1:1.
(d) Pump–probe experiments of O_2:Ar = 2:1 and HCl:Kr = 5:1. In these experiments, the pulse of the pump molecule is separated from the pulse of the probe molecule by a time delay (Δt) of 1–12 s; 10 s after pulsing the probe molecule, a new cycle starts by pulsing the pump molecule and so on.

In the TAP experiments, Kr (Linde, purity 5.0), Ar (Linde, purity 5.0), Cl_2 (Linde, purity 4.0), O_2 (Air Products, purity 5.2), and HCl (Praxair, purity 2.5) were used without further purification. A quadrupole mass spectrometer (RGA 300, Stanford Research Systems) was used for monitoring the transient responses at the reactor outlet of the following atomic mass units (AMUs): 84 (Kr), 70 (Cl_2), 40 (Ar), 36 (HCl), 32 (O_2), and 18 (H_2O). The plotted responses related to experiments (a), (c), and (d) correspond to an average of 10 pulses per AMU in order to improve the signal-to-noise ratio. Prior to that, it was checked that the responses were stable, that is, with invariable intensity and shape during an interval of 20 pulses. The responses of inert gases (Ar, Kr) were not included in the plots as they increase the complexity of the figures while not providing relevant additional information.

3. Results and discussion

3.1. Catalyst characterization

The Ru content in the supported catalysts, determined by ICP–OES, was close to the nominal value of 7 wt.% (Table 1), indicating that the deposition–precipitation of ruthenium as $Ru(OH)_2$ onto the carriers was effective. The X-ray diffraction patterns of the supported catalysts after calcination exhibit characteristic reflections of ruthenium(IV) oxide as well as of the corresponding TiO_2

Table 1
Characterization data of the catalysts.

Catalyst	Ru[a] (wt.%)	S_{BET}[b] (m^2 g^{-1})
RuO_2	76	10
RuO_2/TiO_2-R	6.9	140 (225)[c]
RuO_2/TiO_2-A	6.6	100 (127)
RuO_2/TiO_2-P25	6.7	40 (50)

[a] ICP–OES.
[b] BET method.
[c] Surface area of the carrier in brackets.

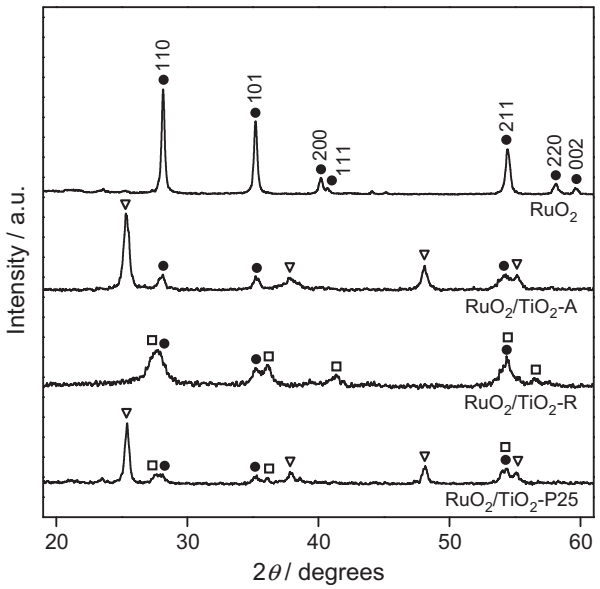

Fig. 2. XRD patterns of the RuO_2-based catalysts. Phases: (●) RuO_2 (JCPDS 40–1290, tetragonal), (□) TiO_2-rutile (JCPDS 78-2485, tetragonal), and (▽) TiO_2-anatase (JCPDS 21-1272, tetragonal). The Miller indices of the main facets of RuO_2 are indicated.

polymorph (Fig. 2). Based on the intensity of the diffraction lines, P25 contains anatase and rutile phases in the expected ratio of 3:1. The position of the RuO_2 and TiO_2-R reflections almost coincide since both materials have the rutile structure [24]. This feature enables the epitaxial growth of RuO_2 on the rutile TiO_2 lattice [25,26]. Table 1 shows the total surface area of the catalysts and supports as determined by N_2 adsorption. The high specific surface area of the rutile (225 $m^2\ g^{-1}$) and anatase (127 $m^2\ g^{-1}$) supports was due to the nanocrystalline nature of the commercial powders, with particle sizes in the range of 25–100 nm according to specifications by the supplier. Confirmation by TEM is provided in Fig. 3. The rutile nanoparticles are elongated (length < 100 nm and thickness in the range of 10–20 nm), while anatase nanoparticles (~25 nm) have a more spherical shape. In contrast, bulk RuO_2 consists of much larger crystallites, giving rise to a total surface area of 10 $m^2\ g^{-1}$. The S_{BET} value of P25 (50 $m^2\ g^{-1}$) is typical of this material [27]. The value of S_{BET} significantly decreases upon ruthenium incorporation in the TiO_2 carriers. The decrease indicates pore blockage by RuO_2, which can be related to the high ruthenium loading and the precipitation method applied to deposit ruthenium. The H_2-TPR profiles of the samples are shown in Fig. 4. The pure carriers were irreducible in the temperature range investigated. The reduction temperature of the RuO_2-supported catalysts, ranging from 425–525 K, agrees with previous studies [28,29]. Two peaks attributed to RuO_2 reduction were observed in all the reduction profiles. This feature has been reported elsewhere [30–32]. Madhavaram et al. [30] attributed the high-temperature reduction peak of bulk RuO_2 to an inhibiting influence of water on the reduction kinetics. However, a heterogeneous distribution of RuO_2 particle sizes may also lead to two reduction peaks [32]. The reduction temperature for the supported systems is noticeably higher than that for bulk RuO_2 due to the interaction between RuO_2 and the carriers. The reduction temperature of RuO_2/TiO_2-R was higher than that of RuO_2/TiO_2-A, and RuO_2/TiO_2-P25 was in between. The stronger interaction of RuO_2 with TiO_2-rutile could be foreseen if epitaxial growth occurs. In this line, detailed microscopy characterization [11] concluded that while RuO_2 is present as nanoparticles on TiO_2-anatase, it is carried as a nanometer-sized thin layer on the rutile polymorph.

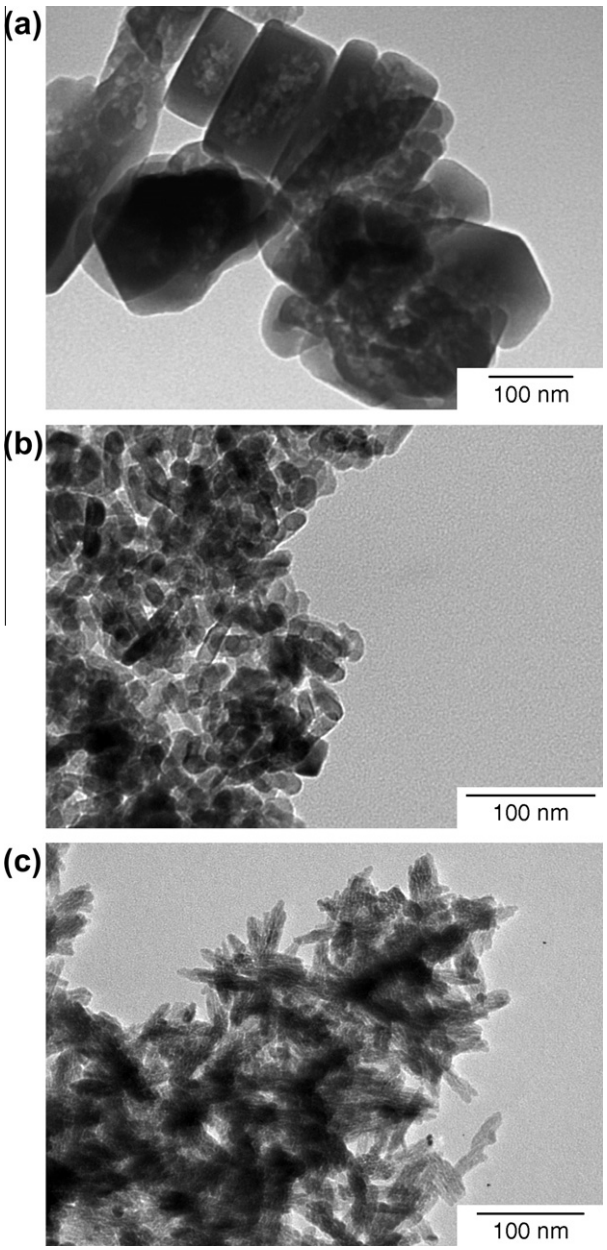

Fig. 3. TEM micrographs of: (a) bulk RuO_2 and the (b) anatase and (c) rutile supports used in this study.

3.2. Catalytic tests

Evaluation of catalysts under relevant Deacon conditions (ambient pressure and high HCl concentration) by academic laboratories is scarce, probably due to the harmful character of the reaction, involving highly corrosive and toxic gases. Herein, the Deacon activity of the catalysts was preliminarily evaluated by temperature-programmed reaction and on-line UV/Vis analysis (typical spectra are shown in Fig. 1c). This transient protocol, reported in our previous study with bulk RuO_2 [13], is suitable for screening purposes. The temperature at which gas-phase Cl_2 evolves from the catalyst by atomic chlorine recombination is indicative of the catalytic activity. Fig. 5 displays the normalized absorbance profiles due to Cl_2 production *versus* the temperature of the catalyst bed. Blank experiments with the pure carriers confirmed that virtually no Cl_2 was produced in the temperature range investigated. RuO_2/TiO_2-R has the lowest onset temperature (T_{10} = 575 K, 10% of

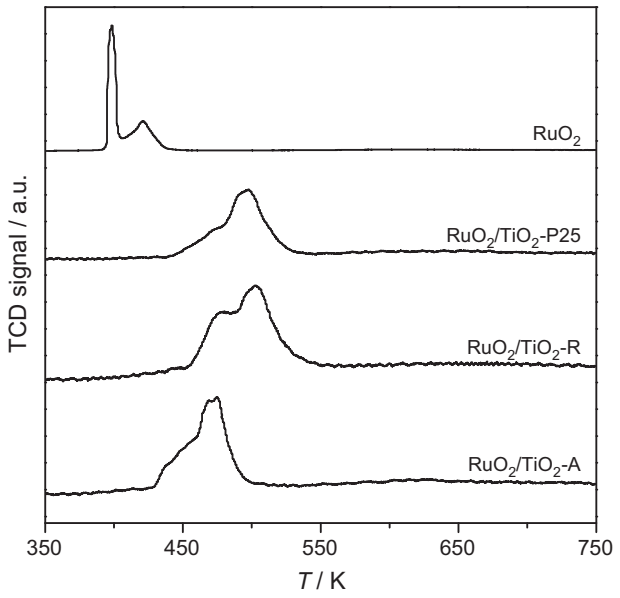

Fig. 4. H_2-TPR profiles of the bulk and supported RuO_2 catalysts.

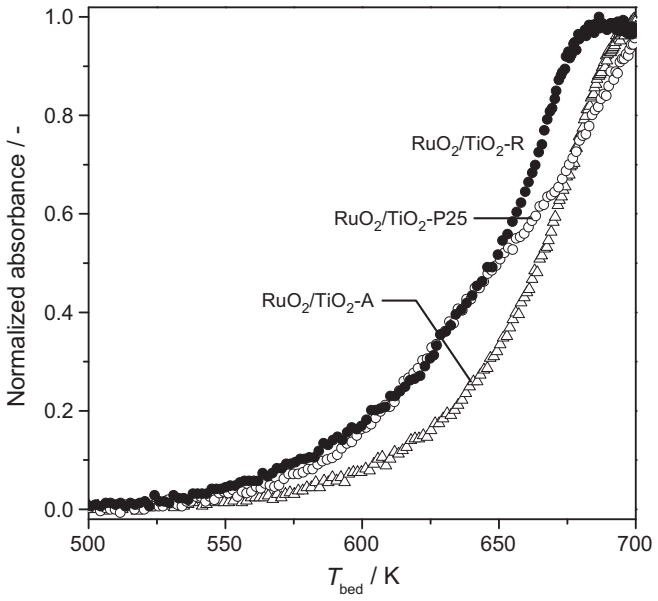

Fig. 5. Light-off curves during temperature-programmed reaction of HCl with O_2 at ambient pressure. The plot shows the normalized absorbance at 330 nm due to Cl_2 *versus* the temperature of the catalyst bed. Conditions: feed mixture of 20 vol.% HCl and 40 vol.% O_2 in N_2, catalyst weight = 0.5 g, and total flow = 166 cm^3 STP min^{-1}.

the total absorbance), closely followed by RuO_2/TiO_2-P25. The activity of RuO_2/TiO_2-A is lower as concluded from the shift of the Cl_2 profiles to higher temperatures. For comparative purposes, the T_{10} determined over bulk RuO_2 (studied by TAP in the next section) was 500 K [13]. The Cl_2 profile of RuO_2/TiO_2-P25 practically coincided with that of RuO_2/TiO_2-R up to 655 K, gradually shifting toward the profiles of RuO_2/TiO_2-A at higher temperatures. This might be related to a deactivation phenomenon occurring during temperature ramping. In order to assess short-term stability, the most active RuO_2/TiO_2-R catalyst was subjected to a second TPR in the Deacon mixture after having cooled down the reactor in N_2. The Cl_2 profile (onset temperature, shape, and absorbance level) matched that of the fresh sample.

Table 2
Deacon activity of selected RuO_2 catalysts in isothermal tests at 573 K for 18 h.

Catalyst	STY[a] (g Cl_2 h^{-1} g_{cat}^{-1})
RuO_2/TiO_2-R	1.19
RuO_2/TiO_2-A	0.83

[a] Space time yield.

The activity during isothermal operation at 573 K for 18 h was measured to quantify the chlorine production of the rutile and anatase-supported RuO_2 catalysts as well as to verify the activity order in Fig. 5. As shown in Table 2, despite the very similar Ru loading, RuO_2/TiO_2-R (STY = 1.19 g Cl_2 h^{-1} g_{cat}^{-1}) was found significantly more active than RuO_2/TiO_2-A (STY = 0.83 g Cl_2 h^{-1} g_{cat}^{-1}). That means 30% higher Cl_2 production over the former catalyst. It should be pointed out that the activity was pretty stable in the duration of the experiment as concluded from the similar STY measured by sampling after 2 or 18 h on stream. These results conclude that the rutile polymorph is preferred to anatase, confirming previous findings by Sumitomo [9–12]. As indicated in some of these references, the epitaxial growth of RuO_2 on TiO_2-R can be a key aspect to attain a highly active (well-dispersed RuO_2 film on the carrier) and stable (strong interaction of the active phase with the carrier) Deacon catalyst. The high surface area of the starting rutile support can also be beneficial for the resulting Deacon activity. We shall not discuss here relationships between the structure of RuO_2 on the different supports and the Deacon activity. This aspect is beyond the scope of this manuscript and would require specific characterization studies to quantify the exposed surface of RuO_2 on the different supports and its morphology. Our prime aim was to investigate the reaction mechanism, and for this purpose, the most active supported system identified was studied in the TAP reactor in fresh and equilibrated forms, along with the pure RuO_2 and TiO_2-R carrier as the references.

3.3. Temporal Analysis of Products

A number of intrinsic features of the TAP reactor make it a powerful technique to investigate the mechanism of HCl oxidation, namely: (i) its millisecond time resolution, (ii) the use of practical catalysts (polycrystalline, supported), (iii) the attainment of isothermal operation, and (iv) safe operation. This is essential attending to the corrosive and toxic compounds involved in the Deacon reaction. Features (iii) and (iv) are possible due to the very low amounts of HCl dosed (in this study, *ca.* 10^{16} molecules per pulse, equivalent to ~20 nmol), giving rise to a negligible adiabatic temperature rise in the shallow catalyst bed and to a very small amount of reaction products in the effluent gas. Nonetheless, several orders of magnitude higher peak pressures are applied in the TAP reactor (in the order of 100 Pa) compared to typical UHV techniques (in the order of 10^{-6} Pa). Accordingly, the Temporal Analysis of Products reactor is uniquely positioned at the boundary of traditional ambient pressure techniques and ultra-high vacuum surface science techniques with respect to catalytic surfaces and pressure regimes [19–22].

3.3.1. Interaction of reactant and product molecules

HCl, O_2, and Cl_2 were individually pulsed at 623 K (reaction temperature) in order to get insights into the interaction of these compounds with the samples. Oxygen generally displayed weak interaction with the catalytic materials attending to the similar transient responses measured over quartz particles as the inert reference (Fig. 6a). The interaction of O_2 is somewhat stronger on bulk RuO_2 as revealed by the broader transient response. This indicates

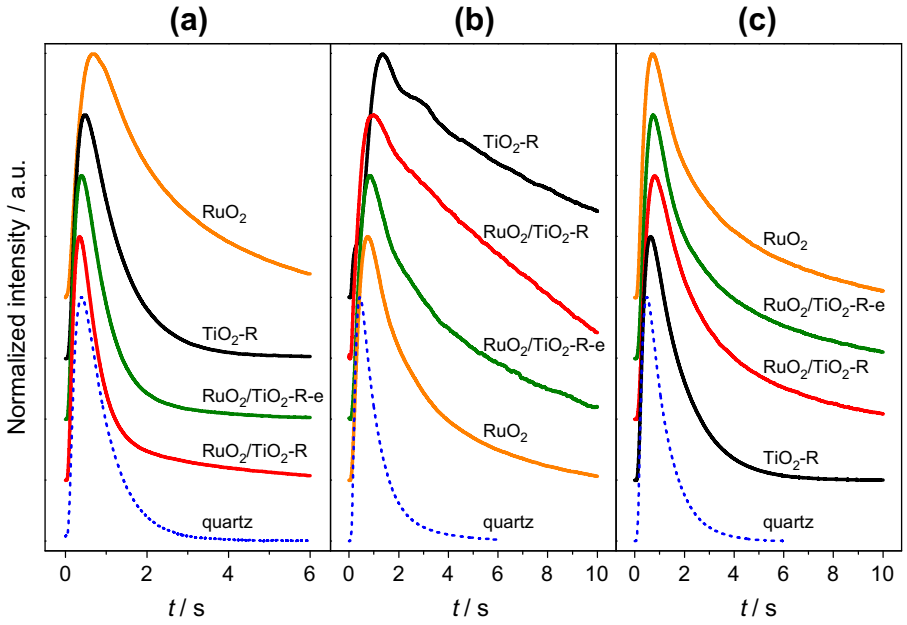

Fig. 6. Normalized transient responses of: (a) O_2, (b) HCl, and (c) Cl_2 pulsed individually over the samples at 623 K.

the occurrence of a reversible adsorption–desorption process. It is well known that gas-phase O_2 dissociatively adsorbs on under-coordinated ruthenium sites (Ru_{cus}) of ruthenium(IV) oxide [13,17,33]. The transient responses of HCl were remarkably broader than those of O_2. The interaction of HCl is strongest on TiO_2-R, since the corresponding transient response is the broadest and the maximum is shifted to longer times with respect to the other samples (Fig. 6b). On the contrary, RuO_2 presents the narrowest HCl response and the position of the maximum is close to that of quartz. The HCl response over TiO_2-R displays a shoulder at *ca.* 3 s, which could correspond to the theoretical prediction of Gleaves et al. [19] for reversible adsorptions in which the desorption constant is significantly smaller than the adsorption one. The weaker interaction of HCl on RuO_2/TiO_2-R-e compared to RuO_2/TiO_2-R, as concluded from the less pronounced tailing over the former sample, is due to the permanent chlorination of the equilibrated catalyst (elaborated in Section 3.3.2), which decreases the driving force for HCl adsorption with respect to the fresh supported catalyst. Finally, the interaction of molecular chlorine on RuO_2 appears to be stronger than on TiO_2-R, based on the broader Cl_2 transient responses of the three RuO_2-containing catalysts is similar and somewhat broader than that over TiO_2-R (Fig. 6c).

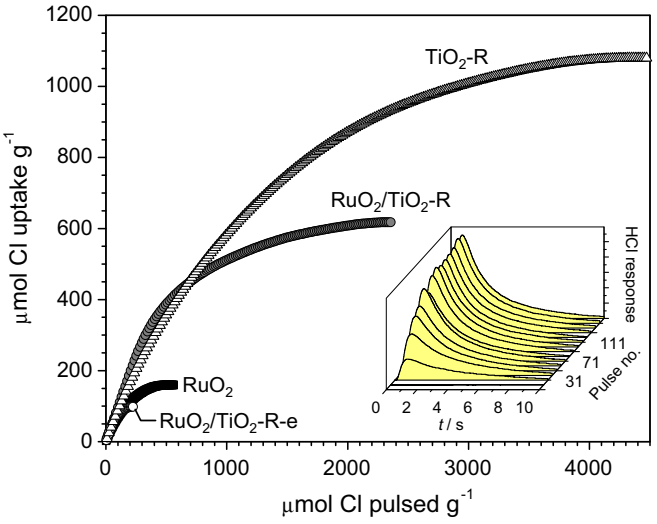

Fig. 7. Chlorination profiles derived from HCl multipulses at 623 K. The inset displays transient HCl responses (every 10 pulses) during chlorination of bulk RuO_2. The intensity of the signal progressively increases with the pulse number until reaching saturation.

3.3.2. Chlorination

The chlorination of bulk RuO_2, the TiO_2-R carrier, and the supported RuO_2/TiO_2-R catalysts in fresh and equilibrated forms was quantitatively determined by means of HCl multipulse experiments at 623 K in the TAP reactor. As illustrated in the inset of Fig. 7 for RuO_2, the samples retained a large fraction of the inlet HCl at low pulse numbers. The intensity of the HCl response progressively increases with the pulse number, and a plateau is reached upon saturation of the material by chlorine. Gas-phase Cl_2 was not detected at the reactor outlet in the course of HCl multipulse experiments. Therefore, the chlorination profiles in Fig. 7 and the quantification in Table 3 were determined by subtraction of the amount of HCl measured at the reactor outlet from the amount of HCl pulsed. As shown later, the introduction of gas-phase O_2 was necessary to monitor distinctive Cl_2 production over the RuO_2-based samples. DFT calculations on RuO_2(1 1 0) concluded that both bridge (O_{br}) and coordinatively unsaturated (O_{cus}) oxygen can dissociate hydrogen chloride with practically no activation barrier [13,14]. The density of O_{cus} under vacuum conditions in the TAP reactor (10^{-5} Pa) at 623 K is expected to be low (<0.25 ML, estimated from *ab initio* thermodynamics [13]). Thus, hydrogen abstraction from HCl is mostly tackled by O_{br}, leading to a bridging hydroxyl group ($O_{br}H$) and a chlorine atom adsorbed on the Ru_{cus} position (Cl_{cus}). Using high-resolution core-level shift spectroscopy on RuO_2(1 1 0) exposed to HCl and annealed at 600 K, Over et al. [15] concluded that Cl_{cus} changes its adsorption site toward the bridge (Cl_{br}), forming a chemically stable oxychloride $RuO_{2-x}Cl_x$. The authors quantified that 50 ± 20% of the bridging oxygen atoms are replaced by chlorine atoms on the chlorinated RuO_2(1 1 0) surface. The percentage of chlorination of Ru_{cus} sites was not discussed in [15]. The Cl_{cus}-to-Cl_{br} transition obviously requires H_2O production *via* recombination of two $O_{br}H$ species,

Table 3
Quantification of the chlorine uptake and chlorination degree of selected samples from multipulse experiments of HCl or Cl_2.

Sample	Pulse	Chlorine uptake		Molar Cl/(Ru or Ti) ratio (–)	
		(μmol Cl g^{-1})	(μmol Cl m^{-2})[a]	Bulk[b]	Surface[c]
RuO_2	HCl	160	16.0	0.021	0.74 (74%)[d]
TiO_2-R	HCl	1080	4.8	0.086	0.23 (23%)
RuO_2	Cl_2	126	12.6	0.017	0.58 (58%)

[a] Based on the total surface area of the samples (Table 1).
[b] Based on the total metal content.
[c] Based on the estimated density of surface metal atoms [34].
[d] The values in brackets denote the percentage of surface chlorination.

forming bare O_{br} and vacancies in the bridge rows where Cl_{br} is stabilized. A broad H_2O signal was detected by mass spectrometry in the course of HCl multipulsing in the TAP reactor.

The chlorine uptake of RuO_2 was 160 μmol Cl g^{-1}, which is equivalent to a molar Cl/Ru_{bulk} ratio of 0.021 (Fig. 7 and Table 3). The $Cl/Ru_{surface}$ ratio was estimated at 0.74, *i.e.* the percentage of surface chlorination of polycrystalline RuO_2 by HCl multipulses in the TAP reactor amounts to ~75%. The Cl/Ru_{bulk} ratio was expressed as the $Cl/Ru_{surface}$ ratio considering the total surface area of the sample (10 m^2 g^{-1}) and the density of surface Ru atoms (1.30×10^{19} atoms $Ru_{surface}$ per m^2). This figure was estimated weighing the density of surface atoms in the main facets of RuO_2 (1 1 0, 1 0 1, 1 0 0, and 0 0 1) according to their relative abundance in the XRD pattern (Fig. 2) [34]. This result confirms that the chlorination of polycrystalline RuO_2 is limited to the surface and is not complete (despite only HCl was pulsed). Good agreement was found with the self-limiting nature of the chlorination process determined by UHV studies on RuO_2(1 1 0) [15], although the TAP-derived degree of surface chlorination over polycrystalline RuO_2 seems to be higher than the UHV-derived over a single crystal. Our previous work [13] also stated the absence of bulk chlorination on RuO_2-based on the limited change in bulk characterization of the sample before and after use in HCl oxidation under flow conditions at 1 bar and 573 K. The ~75% surface chlorination is rather logical considering the above-described mechanistic picture, which is simplistically depicted in Scheme 1. Chlorination starts by HCl activation leading to Cl_{cus} and $O_{br}H$ (steps 1 and 2). $O_{br}H$ species recombine to form O_{br} and H_2O that desorbs (step 3), inducing the change of adsorption site of chlorine from Cl_{cus}-to-Cl_{br} [15]. A third HCl molecule can be activated on the empty cus site, and the proton can be transferred to the regenerated O_{br} (step 4). The chlorination process cannot reach completion since $O_{br}H$ cannot be eliminated from the surface. The Cl coverage is 75% as 3 out of 4 total surface sites in the cell are occupied by atomic chlorine. It is beyond the scope of Scheme 1 to describe on a molecular level the transport of protons and diffusion of atomic species on the surface, but namely to illustrate the full chlorination of the catalyst surface is indeed unlikely.

As seen in Fig. 7, the rutile carrier experienced significant chlorination in HCl multipulse experiments. Per gram of sample, the chlorine uptake of TiO_2-R (1080 μmol Cl g^{-1}) was *ca.* 7 times higher than that of RuO_2 (160 μmol Cl g^{-1}). At first sight, this result denotes great differences between the samples. However, the total surface area of rutile is more than 25 times higher than that of

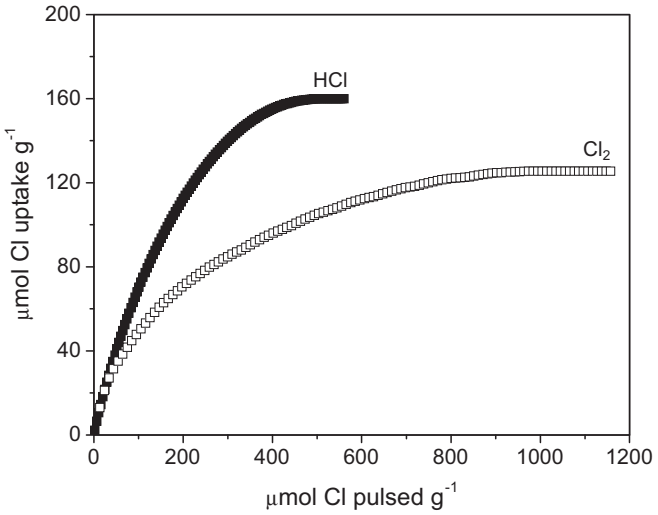

Fig. 8. Comparison of the chlorination profiles of RuO_2 by Cl_2 and HCl multipulses in the TAP reactor at 623 K.

ruthenium dioxide (Table 1). Therefore, a more appropriate comparison arises from the normalization of the chlorine uptake by the exposed surface area (fourth column in Table 3). Following this, the surface of RuO_2 presents more than a 3-fold increased chlorination by HCl with respect to TiO_2. As explained earlier for RuO_2, the percentage of surface chlorination of TiO_2-R was estimated at 23%. This result unequivocally demonstrates that TiO_2-R is able to abstract hydrogen from HCl in the absence of gas-phase O_2. The strong interaction of HCl over the high surface area TiO_2-R used in this study was concluded from the very broad and highly delayed responses obtained in single-pulse experiments (Fig. 6b). However, the surface of RuO_2 chlorinates to a larger extent, strongly suggesting the stronger basic character of O_{br} in RuO_2 compared to that in TiO_2-R. The oxygen basicity is expected to be directly linked with the ability of the material toward chlorination. The lower chlorination of TiO_2-R might be due to the difficult desorption of H_2O. Despite this feature, we have experimentally verified that TiO_2 is inactive in the Deacon reaction, which is related to its inability to dissociate O_2 (*i.e.* catalyst reoxidation does not occur) [16]. In line with this, the transient responses of O_2 on TiO_2-R and inert quartz particles were very similar (Fig. 6a). The chlorine uptake of the fresh supported RuO_2/TiO_2-R catalyst was also relatively high. This can be expected attending to the relatively high surface area of the sample (140 m^2 g^{-1}) and the chlorination of both RuO_2 and TiO_2-R components. The most interesting observation is that the chlorine uptake of the equilibrated RuO_2/TiO_2-R catalyst experienced a 6-fold decrease with respect to the fresh counterpart. This indicates the occurrence of substantial permanent chlorination of the supported sample after isothermal tests in the Deacon mixture at ambient pressure.

Multipulse experiments of Cl_2 at 623 K were also conducted over RuO_2 in order to compare the chlorinating ability of HCl and Cl_2. The chlorination profiles using both Cl-containing molecules are plotted in Fig. 8. The RuO_2 surface is also chlorinated by Cl_2 but to a lesser extent compared to HCl (58% *versus* 74%, Table 3). The differences in slope clearly indicate that HCl is easier to

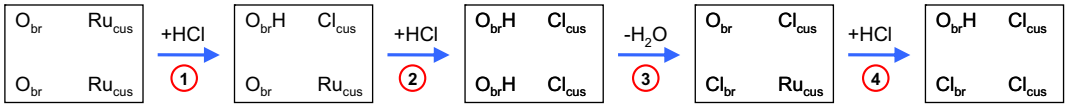

Scheme 1. Representation of the successive chlorination of a RuO_2 cell by HCl.

activate on RuO_2 than Cl_2, leading to a much faster chlorination kinetics. However, the significant chlorine uptake by splitting of the Cl_2 molecule coupled to its strong adsorption over the saturated catalyst (Fig. 6) strongly suggest that the Deacon process on ruthenium-based catalyst should suffer from product inhibition.

The aforementioned results highlight that the TAP reactor in multipulse mode is a powerful tool to determine the degree of chlorination of RuO_2 and TiO_2-based samples, which is an important aspect in the design and understanding of Deacon catalysts. It is not straight forward to identify alternative techniques able to probe the chlorine uptake of solid samples by HCl or Cl_2 at a relatively high temperature.

3.3.3. Pulses of HCl + O_2 mixture

Fig. 9 shows the TAP responses on pulsing of a mixture of HCl and O_2 over RuO_2 at 623 K. The transients over the supported catalysts were qualitatively very similar and are not shown for conciseness. This experiment was carried out after HCl multipulsing described in the previous section and therefore the catalysts were stabilized in a partially chlorinated form. An important conclusion from Fig. 9 is the detection of reaction products (Cl_2 and H_2O) at the reactor outlet, which demonstrates the suitability of the TAP reactor to study the Deacon reaction. In order to monitor gas-phase Cl_2, the introduction of O_2 together with HCl is required. Hydrogen abstraction from HCl by structural oxygen species in bridge positions is very favorable, but not the Cl_2 evolution. The recombination of two adjacent chlorine atoms to gas-phase Cl_2 on the clean RuO_2(1 1 0) surface is highly endothermic (1.8 eV for $Cl_{cus} + Cl_{cus}$ and 3.2 eV for $Cl_{cus} + Cl_{br}$) [13] and is regarded as the rate-determining step of HCl oxidation [13,14]. The relatively broad Cl_2 response in Fig. 9 is indicative of the impeded Cl_2 evolution. However, the time of the maximum (t_{max}) of the Cl_2 response coincides with the maximum of the reactants' responses. This suggests that recombination of adjacent chlorine atoms is not the limiting step in energetic terms, but rather the desorption of molecular chlorine. The latter provokes the tailing of the response. DFT calculations [13] have shown that an increased coverage on the cus row of RuO_2(1 1 0) significantly lowers the energy required for $Cl_{cus} + Cl_{cus}$ recombination and Cl_2 desorption, even below 1.3 eV for O_{cus} coverage of 0.5 on a $p(4 \times 1)$ cell. HCl pulsing (Section 3.3.2) did not produce gas-phase Cl_2 since the coverage by O_{cus} is very low, rendering a very high barrier for chlorine desorption. However, the simultaneous pulsing of HCl and O_2 increases the coverage by O_{cus}, which assists the Deacon process in abstracting hydrogen from HCl and, most important, in decreasing the Cl_2 desorption barrier. The influence of the lifetime of O_{cus} species on the net Cl_2 production has been addressed in the next section by means of pump–probe experiments.

A very interesting observation in Fig. 9 is the very broad and low-intensity signal of H_2O. The inset of this figure shows the responses of H_2O and Cl_2, which have been normalized in order to better compare their shapes. H_2O evolution is even more impeded than Cl_2 evolution under TAP conditions: the water response was significantly shifted to longer times ($\Delta t_{h/2} \sim 1$ s) with respect to the chlorine response and also the position of the maximum (t_{max}). This step was not been regarded as critical in the overall reaction mechanism in previous UHV and DFT studies [13–16]. The aforesaid analysis of the TAP responses when pulsing a HCl + O_2 mixture at a relevant Deacon temperature concludes differently. H_2O desorption is a prominent step in the overall mechanism as it regenerates an active site.

Seminal work by Over et al. [14] stated that the HCl oxidation follows a one-dimensional Langmuir–Hinshelwood mechanism; 'one-dimensional' refers to the fact that Cl_2 production happens in the direction of the Ru_{cus} row. However, the transfer of the proton from HCl to O_{br} is a relevant step too. Overall, it is more appropriate to state that the reaction follows a two-dimensional mechanism, implying that Cl_2 production namely occurs in the Ru_{cus} row, but other steps can occur perpendicularly to this row, *i.e.* involving species in bridge and cus positions.

3.3.4. Pump–probe experiments

Pump–probe experiments with O_2 and HCl exchanging their roles (O_2 pump and HCl probe or HCl pump and O_2 probe) were carried out at 623 K over RuO_2, RuO_2/TiO_2-R, and RuO_2/TiO_2-R-e after pulsing the HCl + O_2 mixture. The time delay between the pump and probe pulses (Δt) was varied in the 1–12 s range, allowing to study the influence of the pump molecule coverage. The consecutive cycles were linked in such a way that the time elapsed between the probe pulse and the pump pulse in the next cycle was always of 10 s. Therefore, the coverage of the probe molecule at the beginning of the cycle is very low, since after 10 s the probe pulse has almost wholly eluted, as can be deduced from Fig. 6.

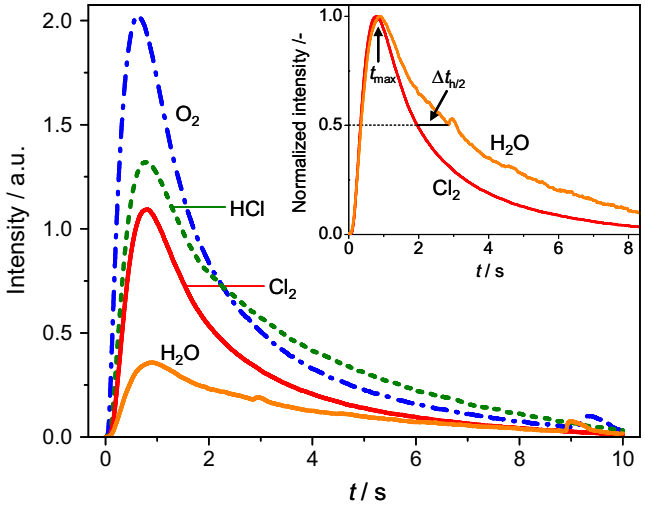

Fig. 9. Transient responses of reactants and products on pulsing a mixture of HCl:O_2 = 2:1 over RuO_2 at 623 K. Inset: normalized transient responses of reaction products. Prior to the experiment, the catalyst was subjected to HCl multipulses at 623 K (Fig. 7) and therefore was stabilized in the oxychloride form.

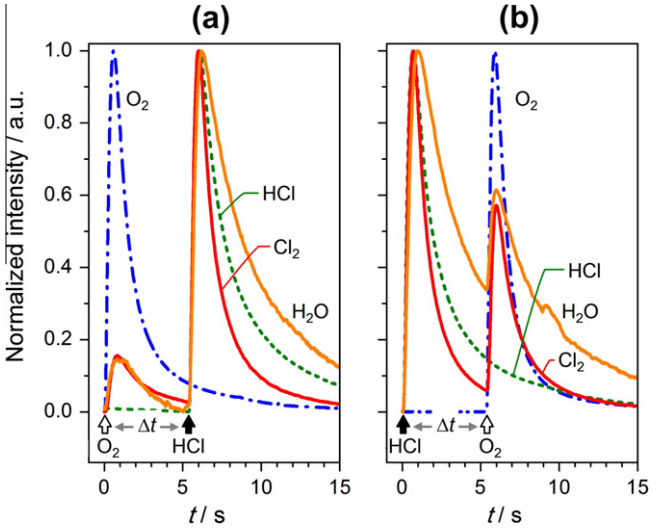

Fig. 10. Normalized transient responses in pump–probe experiments over RuO_2 at 623 K: (a) O_2 pump and HCl probe and (b) HCl pump and O_2 probe. The time delay (Δt) between pulses was 5 s.

Fig. 10 illustrates typical results obtained in pump–probe experiments. Reaction products, Cl_2 and H_2O, are observed in both O_2 and HCl pulses, no matter the order of pulsing. H_2O responses are broader than those of Cl_2 in most cases, supporting the difficulty of the H_2O desorption step and its prominence in the overall mechanism. This conclusion was already derived from the experiments with the HCl + O_2 mixture discussed in the previous section. The HCl responses were broader than those of Cl_2.

More insights into the mechanism can be obtained from a deeper analysis of Cl_2 responses in pump–probe experiments at different time delays, as depicted in Fig. 11 for RuO_2, RuO_2/TiO_2-R, and RuO_2/TiO_2-R-e. A decrease of Cl_2 production as Δt increases can be clearly noticed, that is, as the coverages of both O_2 (Fig. 11a) and HCl (Fig. 11b) decrease, indicating that the reaction occurs in the presence of adsorbed species in all cases. Fig. 11 also shows that there is an essential change between RuO_2/TiO_2-R (fresh) and RuO_2/TiO_2-R-e (equilibrated) in the general pattern of Cl_2 responses in pump–probe experiments. RuO_2/TiO_2-R, similarly to RuO_2, tends to produce more Cl_2 in the HCl pulse than in the O_2 pulse, the opposite being true for RuO_2/TiO_2-R-e. In addition, the total amount of Cl_2 produced was much higher for RuO_2/TiO_2-R-e (Fig. 12). Therefore, the equilibration process, *i.e.* the sustained continuous-flow Deacon reaction at ambient pressure, undertakes structural changes in the catalyst that drastically increase its activity and alter the mechanism. The equilibrated catalyst is rich in active surface chlorine species, able to produce important amounts of Cl_2 at O_2 pulsing, even after the HCl pulse has eluted almost completely. The formation of the oxychlorides that provoke such a transformation in the catalytic performance is not merely a degree of chlorination issue, since the equilibrated RuO_2/TiO_2-R-e catalyst can be further chlorinated (to a limited extent) in TAP conditions (Section 3.3.2.). Nevertheless, a fresh catalyst (RuO_2/TiO_2-R)

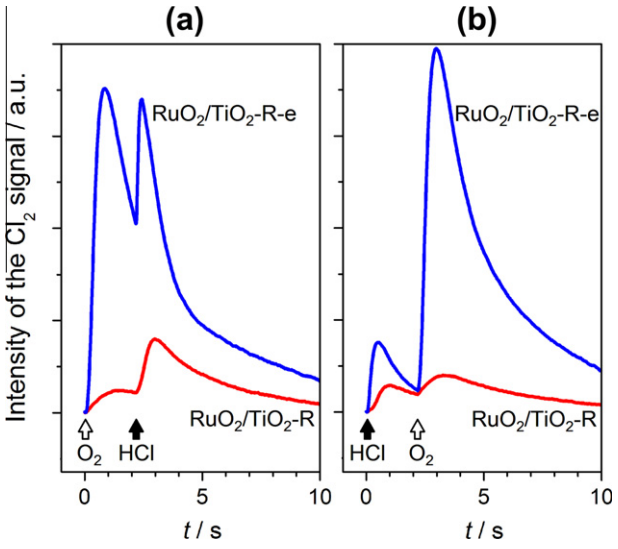

Fig. 12. Transient responses of Cl_2 in pump–probe experiments over RuO_2/TiO_2-R and RuO_2/TiO_2-R-e at 623 K: (a) O_2 pump and HCl probe and (b) HCl pump and O_2 probe. The time delay (Δt) between pulses was 2 s.

chlorinated to saturation in the TAP leads to a completely different net Cl_2 production, strongly suggesting that the structure and/or composition of the oxychloride species differ depending on chlorination conditions. This is a proof of the dynamic nature of rutile-supported RuO_2 catalysts, which heavily depend on their working conditions history.

Further understanding of the mechanism can be attained by means of Fig. 13, which comes from proper quantification of the

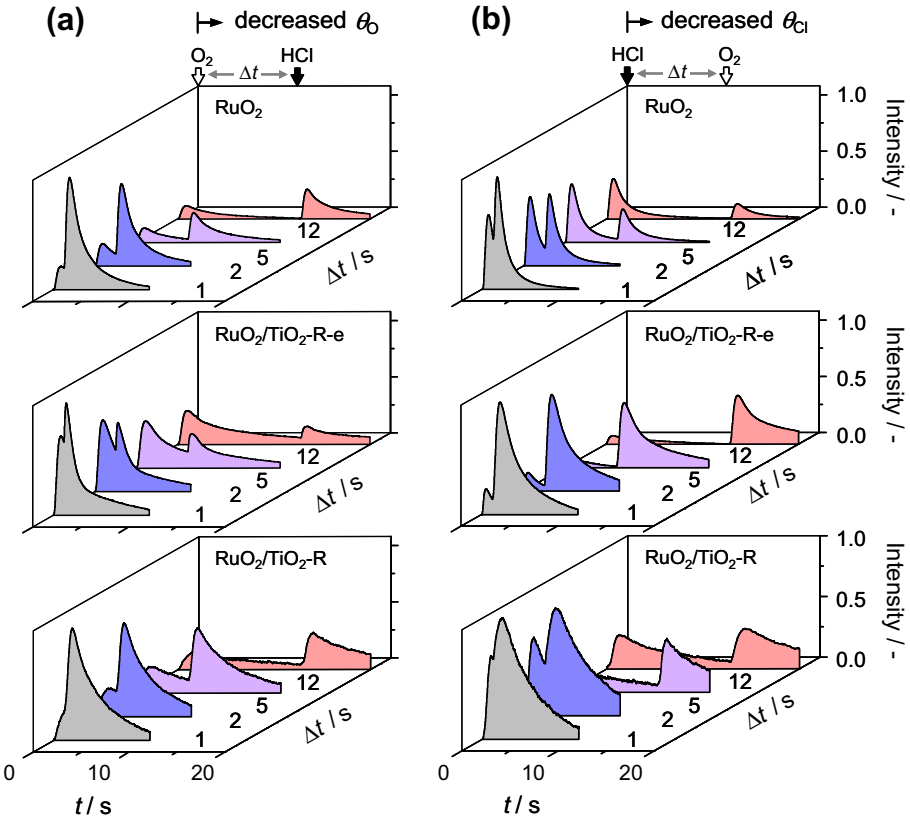

Fig. 11. Transient responses of Cl_2 over the catalysts in pump–probe experiments of: (a) O_2 pump and HCl probe and (b) HCl pump and O_2 probe at different time delays and 623 K. In all cases, the responses were height-normalized to the intensity of the response at Δt = 1 s.

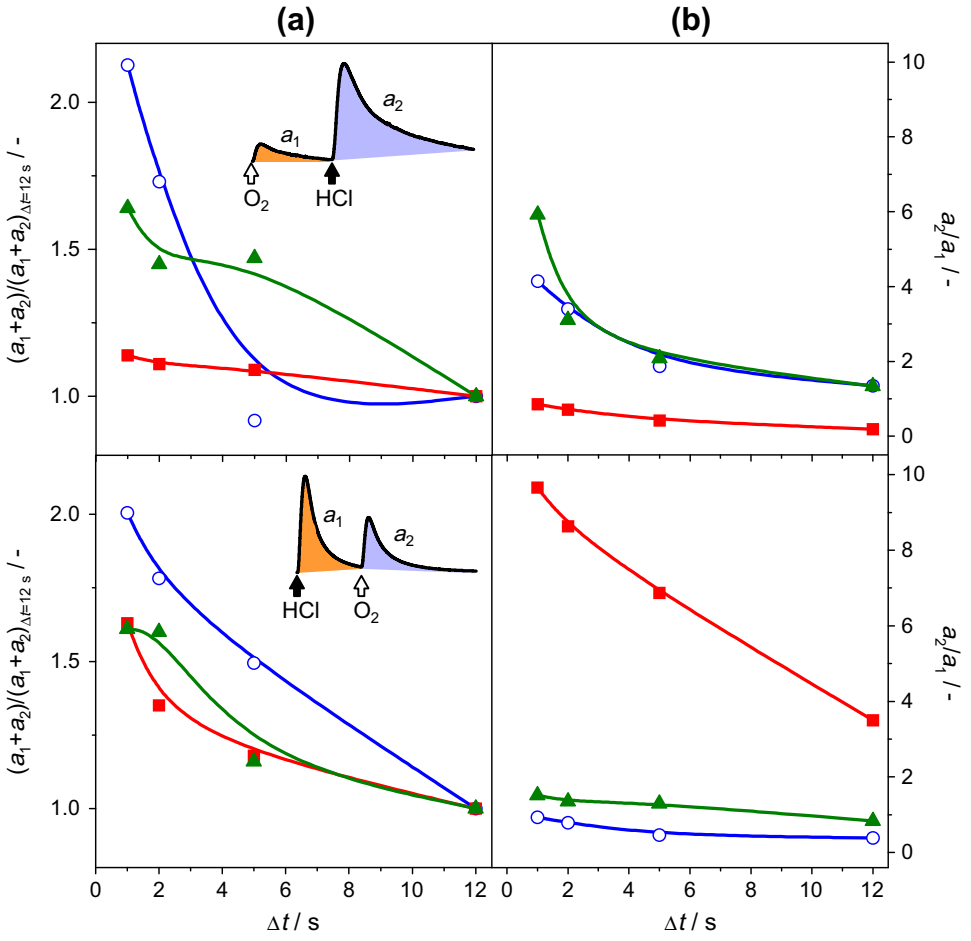

Fig. 13. Calculations related to Cl_2 production derived from Fig. 11 over (○) RuO_2, (▲) RuO_2/TiO_2-R, and (■) RuO_2/TiO_2-R-e. The total Cl_2 production in (a), defined as the sum of the areas in the pump (a_1) and probe (a_2) pulses, was relative to the experiment at Δt = 12 s. The ratio of Cl_2 produced in the probe pulse and in the pump pulse (a_2/a_1) is shown in (b).

data provided in Fig. 11, *i.e.* the analysis of the Δt effect on both the total Cl_2 production (Fig. 13a) and the ratio between the Cl_2 formed in the pump and probe pulses (Fig. 13b). When O_2 is the pump molecule (Fig. 13a, top), increasing the Δt from 1 s to 12 s induces a decrease in Cl_2 production of *ca.* 110% for RuO_2, 60% for RuO_2/TiO_2-R, and 15% for RuO_2/TiO_2-R-e. This is a direct evidence of the participation of relatively short-lifetime adsorbed oxygen species in the reaction over RuO_2 and RuO_2/TiO_2-R. The low production of Cl_2 in the O_2 pulse is also an indication that oxygen cannot activate the surface chlorine species on these two catalysts. For RuO_2/TiO_2-R-e, the situation is quite different; the dependence of Cl_2 production on the oxygen coverage is smoother because Cl_2 is produced to a larger extent in the first pulse (O_2), implying that, contrarily to RuO_2 and RuO_2/TiO_2-R, significant amounts of chlorine species over its surface can be activated by oxygen. When HCl is the pump molecule (Fig. 13a, bottom), there is a marked decrease in the Cl_2 production with Δt for the three catalysts: *ca.* 100% for RuO_2 and 60% for both RuO_2/TiO_2-R and RuO_2/TiO_2-R-e. This implies that Cl_2 is produced mostly from adsorbed chlorine, particularly in the case of pure RuO_2. In addition to the overall Cl_2 produced (Fig. 13a), the ratio of Cl_2 produced between probe and pump pulses (a_2/a_1), yields a better distinction of the catalysts with regard to the coverage effect of the reactants, as shown in Fig. 13b. There are clearly two patterns: sharply decreasing plots with a_2/a_1 well above 1 and smoothly decreasing plots with a_2/a_1 roughly in the 0–1 range. Every catalyst shows the two patterns depending on the pulsing order: *i.e.* RuO_2/TiO_2-R-e decreases smoothly when O_2 is the pump and decreases sharply when HCl is the pump, the opposite holds for RuO_2/TiO_2-R and RuO_2. The fact that one catalyst shows one pattern or the other lies on its capability of producing relatively important amounts of Cl_2 under very low partial pressures of either HCl (RuO_2/TiO_2-R-e) or O_2 (RuO_2 and RuO_2/TiO_2-R), and therefore on the existence of long-lifetime active chlorine and oxygen species respectively on the catalytic surface. Accordingly, a plot like that of RuO_2/TiO_2-R-e (HCl probe) or those of RuO_2 and RuO_2/TiO_2-R (O_2 probe) in Fig. 13b is a fingerprint of the presence of long-lifetime species related to the probe molecule.

Summarizing, the overall picture of the mechanism obtained in these pump–probe experiments shows that the reaction occurs predominantly between adsorbed species when the coverages of HCl and O_2 are high, which is the situation of practical interest. The experiments in which the coverage of one of the reactants is low have shown that the surface chemistry of RuO_2/TiO_2-R-e allows the formation of relatively important amounts of Cl_2 at very low partial pressures of HCl, while RuO_2 and RuO_2/TiO_2-R are able to do the same at very low partial pressures of O_2.

4. Conclusions

The Temporal Analysis of Products (TAP) reactor was successfully used to investigate the HCl oxidation to Cl_2 over practical catalysts (polycrystalline RuO_2 and supported RuO_2/TiO_2 catalysts).

Several intrinsic features of this transient pulse technique make it a unique tool to study the mechanism of this complex and experimentally demanding reaction. Catalytic tests in a flow reactor at ambient pressure demonstrated that rutile was the preferred TiO_2 polymorph to support the RuO_2 phase. HCl multipulsing in the absence of O_2 leads to chlorination of the samples with no detectable gas-phase Cl_2 production. The chlorination is limited to the surface and is not complete, leading to a stable oxychloride ($RuO_{2-x}Cl_x$). The latter is the effective species catalyzing HCl oxidation to Cl_2. The degree of surface chlorination of RuO_2 by HCl was estimated at 74%, significantly higher compared to that of TiO_2-rutile (23%). This suggests the stronger basic character of oxygen on ruthenium dioxide. RuO_2 can also activate the Cl_2 molecule, but the chlorination kinetics is slower compared to HCl and the degree of surface chlorination amounted to 58%. The chlorine uptake of the fresh supported catalyst per gram of sample largely exceeded that of pure RuO_2, namely due to chlorination of the high surface area rutile carrier. Upon equilibration at ambient pressure under Deacon conditions, the chlorine uptake of the supported catalyst abruptly decreased due to permanent chlorination. Pulsing of a mixture of O_2 and HCl over the catalysts revealed that both gas-phase Cl_2 evolution and H_2O desorption are impeded processes. Pump–probe experiments between O_2 and HCl (or in the reverse order) concluded the reaction takes place predominantly in the presence of adsorbed species, since the net Cl_2 production is highly influenced by both the oxygen and chlorine coverage. The small amounts of Cl_2 detected at very low coverages are attributed to surface lattice species. The equilibration procedure (ambient or TAP conditions) impacts on the reaction mechanism and the Cl_2 production, suggesting that oxychloride phases with different structure and/composition are formed. These results give account on the reaction complexity due to the highly dynamic state of the catalyst surface. The Deacon process on $RuO_{2-x}Cl_x$-based catalysts can be mostly described by a Langmuir–Hinshelwood scheme with a minor Mars–van Krevelen contribution.

Acknowledgments

We thank Bayer MaterialScience AG for permission to publish these results. Dr. L. Durán Pachón and R.P. Marín are acknowledged for their input in preparation and characterization of the samples by XRD and H_2-TPR. Dr. D. Teschner (FHI Berlin) and Dr. N. López (ICIQ Tarragona) are acknowledged for fruitful discussions.

References

[1] S. Motupally, D.T. Mah, F.J. Freire, J.W. Weidner, Electrochem. Soc. Interface 7 (3) (1998) 32.
[2] H. Deacon, US Patent 85,370, 1868.
[3] H. Deacon, US Patent 165,802, 1875.
[4] A.J. Johnson, A.J. Cherniavsky, US Patent 2542,961, 1951.
[5] F. Wattimena, W.M.H. Sachtler, Stud. Surf. Sci. Catal. 7 (1981) 816.
[6] H. Itoh, Y. Kono, M. Ajioka, S. Takezaka, M. Katzita, US Patent 4803,065, 1989.
[7] T. Kiyoura, Y. Kogure, T. Nagayama, K. Kanaya, US Patent 4822,589, 1989.
[8] T. Yasuaki, Stud. Surf. Sci. Catal. 92 (1995) 41.
[9] T. Hibi, H. Nishida, H. Abekawa, US Patent 5871,707, 1999.
[10] T. Hibi, T. Okuhara, K. Seki, H. Abekawa, H. Hamamatsu, WO 01/10550, 2001.
[11] K. Iwanaga, K. Seki, T. Hibi, K. Issoh, T. Suzuta, M. Nakada, Y. Mori, T. Abe, Sumitomo Kagaku 1 (2004) 4.
[12] K. Seki, Shokubai 51 (2009) 540.
[13] N. López, J. Gómez-Segura, R.P. Marín, J. Pérez-Ramírez, J. Catal. 255 (2008) 29.
[14] S. Zweidinger, D. Crihan, M. Knapp, J.P. Hofmann, A.P. Seitsonen, C.J. Weststrate, E. Lundgren, J.N. Andersen, H. Over, J. Phys. Chem. C 112 (2008) 9966.
[15] D. Crihan, M. Knapp, S. Zweidinger, E. Lundgren, C.J. Weststrate, J.N. Andersen, A.P. Seitsonen, H. Over, Angew. Chem. Int. Ed. 47 (2008) 2131.
[16] F. Studt, F. Abild-Pedersen, H.A. Hansen, I.C. Man, J. Rossmeisl, T. Bligaard, ChemCatChem 2 (2010) 1.
[17] H. Over, Y.D. Kim, A.P. Seitsonen, S. Wendt, E. Lundgren, M. Schmid, P. Varga, A. Morgante, G. Ertl, Science 287 (2000) 1474.
[18] Y. Wang, K. Jacobi, W.-D. Schöne, G. Ertl, J. Phys. Chem. B 109 (2005) 7883.
[19] J.T. Gleaves, G.S. Yablonsky, P. Phanawadee, Y. Schuurman, Appl. Catal. A 160 (1997) 55.
[20] J. Pérez-Ramírez, E.V. Kondratenko, Catal. Today 121 (2007) 160.
[21] J.T. Gleaves, G. Yablonsky, X. Zhenga, R. Fushimi, P.L. Mills, J. Mol. Catal. A: Chem. 35 (2010) 108.
[22] G.S. Yablonsky, M. Olea, G.B. Marin, J. Catal. 216 (2003) 120.
[23] S.O. Shekhtman, G.S. Yablonsky, S. Chen, J.T. Gleaves, Chem. Eng. Sci. 54 (1999) 4371.
[24] D.B. Rogers, R.D. Shannon, A.W. Sleight, J.L. Gillson, Inorg. Chem. 8 (1969) 841.
[25] G.A. Rizzi, A. Magrin, G. Granozzi, Surf. Sci. 443 (1999) 277.
[26] G.X. Miaoa, A. Gupta, G. Xiao, A. Anguelouch, Thin Solid Films 478 (2005) 159.
[27] T. Ohno, K. Sarukawa, K. Tokieda, M. Matsumura, J. Catal. 203 (2001) 82.
[28] H. Liu, E. Iglesia, J. Phys. Chem. B 109 (2005) 2155.
[29] T. Mitsui, K. Tsutsui, T. Matsui, R. Kikuchi, K. Eguchi, Appl. Catal. B 81 (2008) 56.
[30] H. Madhavaram, H. Idriss, S. Wendt, Y.D. Kim, M. Knapp, H. Over, J. Aβmann, E. Löffler, M. Muhler, J. Catal. 202 (2001) 296.
[31] J. Assmann, V. Narkhede, L. Khodeir, E. Löffler, O. Hinrichsen, A. Birkner, H. Over, M. Muhler, J. Phys. Chem. B 108 (2004) 14634.
[32] I. Balint, A. Miyazaki, K.-i. Aika, React. Kinet. Catal. Lett. 80 (2003) 81.
[33] S. Wendt, M. Knapp, H. Over, J. Am. Chem. Soc. 126 (2004) 1537.
[34] The total density of surface Ru atoms (cus + bridge) of RuO_2(1 1 0) is 9.9×10^{18} atoms m^{-2}. The density of surface Ru atoms on the other facets is higher, *i.e.* 1.58×10^{19} atoms m^{-2} on (1 0 1), 1.39×10^{19} atoms m^{-2} on (1 0 0), and 1.92×10^{19} atoms m^{-2} on (0 0 1). These values were determined from the cell parameters of each plane. Taking into account the relative abundance of these four facets in the XRD pattern of Fig. 2 (51% of (1 1 0), 38% of (1 0 1), 8% of (1 0 0), and 3% of (0 0 1)) the density of ruthenium atoms in the polycrystalline RuO_2 sample can be estimated at 1.30×10^{19} atoms m^{-2}.